Nonlinear Reduced Order Modeling of a Curved Axi-symmetric Perforated Plate: Comparison with Experiments

David A. Ehrhardt
Research Assistant
Department of Mechanical Engineering, University of Bristol
david.ehrhardt@bristol.ac.uk

Matthew S. Allen
Associate Professor
Department of Engineering Physics, University of Wisconsin-Madison

Abstract

Structures undergoing large amplitude deformations usually include nonlinear strain-displacement relationships defining a geometric nonlinearity. This type of nonlinearity can be observed in structures with fixed boundary conditions where mid-plane stretching occurs at large deflections. When considering the dynamic response of the structure under these circumstances, the once uncoupled linear normal modes become coupled at large response amplitudes changing the characteristic deformation shape as the fundamental frequency of vibration changes. Therefore, the development of nonlinear reduced order models to predict the dynamic response of such structures should account for any potential coupling between the linear normal modes. In this context, a structures' nonlinear normal modes provide a compact characterization of modal coupling in the structural response in nonlinear regimes. This work uses experimentally measured and numerically calculated nonlinear normal modes for a curved axi-symmetric perforated plate to build a nonlinear reduced order model and gain insight to the underlying modal coupling. A comparison is made between two models and corresponding experimental structures to assess the model's ability to describe the modal coupling.

Keywords: nonlinear normal modes, circular plate

1. Introduction

Geometric nonlinearity manifests in structures experiencing large amplitude deformations where axial stretching causes coupling between in-plane and out-of-plane motion. The coupled in-plane and out-of-plane motion also leads to a coupling of the underlying linear normal modes of vibration. Since established structural design techniques rely on uncoupled linear modes of vibration, new methods are sought to address nonlinear behavior while preserving the simplicity of the traditional design and test paradigms. Geometric nonlinearity is of particular interest in thin, constrained structures since nonlinear deformations can occur in the elastic region of the material. Therefore, the design of such structures can be beneficial because the nonlinearity couples the linear modes, spreading energy into other modes that would otherwise not be excited. In other scenarios, the unexpected deformations in these modes may cause large stresses and unexpected failures. The examination and understanding of the structural response and modal coupling at large amplitudes of deformations provides insight to the structure's design.

This work uses the nonlinear normal mode (NNM) concept as a tool for testing and modeling of nonlinear structures. A structure's NNMs provide insight into the dynamic response and modal coupling at large amplitudes of deformation [1]. The presentation of NNMs in frequency-energy plots allow the entire structural deformation to be presented compactly. However, due to the spatial complexity of the expected deformations, an examination of the full field response is beneficial to understanding the underlying modal coupling.

Several advances in recent years have begun to make nonlinear modeling and testing for model updating a reality for practical structures. Peeters et al. [2] recently presented a technique to compute NNMs based on numerical integration and continuation which has proven effective for computing the NNMs of a structure with hundreds of degrees of freedom so long as the nonlinearities are localized. Allen, Kuether & Deaner [3, 4] recently extended that approach to structures with geometric nonlinearities that are modeled within commercial finite element software. An alternative to the calculation of NNMs has also been established where NNMs are calculated using nonlinear reduced order models which are generated with commercial finite element software [3, 5]. Although less computationally expensive than the full order model, the selection of the correct modal basis can be troublesome. The selection of the correct modal basis can be aided with the use of short time simulations of the full order model or an exploration of the experimental structure.

There are two approaches that have been successfully implemented in the experimental determination of NNMs. Both have relied on a stepped sine force appropriation technique to force a structure to vibrate in only one NNM [6]. The first

method makes the assumption that the free decay of a structure that is initiated on a NNM should follow the NNM for lightly damped structures. Therefore, once an NNM is isolated, the excitation can then be removed and the response would then presumably decay along the NNM. Peeters et al [7] applied this technique to a beam with a local nonlinearity at one end with good results. Additionally, Ehrhardt [8] also performed a free decay experiment on a clamped-clamped beam with geometric nonlinearity. It was found that for NNMs with a single dominant linear mode, the free decay traced the NNM well; however, for an NNM with coupled linear modes (i.e. the first and third mode) the free decay does not match the expected NNM. Kuether & Allen proposed a variant on this technique that was used to compute NNMs [9], but also has been extended to measure an NNM by progressively adjusting the excitation frequency and amplitude repeatedly using force appropriation to isolate NNMs. One additional benefit to this measurement of NNMs is the ease of implementation of full-field measurement techniques such as 3D digital image correlation (3D-DIC) or continuous-scan laser Doppler vibrometry (CSLDV) [10].

This work uses manually tuned stepped-sine testing to find the first nonlinear normal mode of the of two curved axi-symmetric plates over a range of excitation amplitudes. The methods developed in [3, 4] are then used to compute the NNMs of the geometrically nonlinear structure using a detailed finite element model, and then the experimentally estimated nonlinear modes are compared with those computed from the model to determine how the model should be updated. This investigation focuses on the first symmetric mode of two different axi-symmetric plates.

2. Numerical Model and Experimental Structure

2.1 Finite Element Model

In this investigation, finite element models (FEMs) were built using the nominal measured geometries of the perforated plate described in the next section. It is assumed that the welded boundary between the plate and steel cylinder provide fixed boundary conditions in all models. The goal of modeling in this work is to determine an equivalent model that can capture the dynamic behavior of the structure. If a detailed representation of the stress distribution is needed, a very fine mesh would be required in order to model each of the perforations. However, Jhung and Jo [11] found that a perforated plate behaves dynamically identical to a non-perforated plate of the same dimensions, as long as the elastic properties are adjusted appropriately. Hence, the reduced elastic modulus and density were calculated based on the perforation geometry as detailed by Jhung and Jo [11], which for the triangular perforation pattern of this plate yields a new elastic modulus of 1.68 GPa and density of 5120 kg/m^3. The resulting meshed Abaqus model is shown in Fig. 2, and has 1440 S4R shell elements. The elastic modulus was later updated so numerically predicted and experimentally measured natural frequencies match. The reduced density was not updated because it can be computed from the geometric properties of the perforations (ex. size of hole and count) and hence should be quite accurate. On the other hand, the effective modulus is dependent on any residual stresses from the addition of perforations, or imperfections of the perforation location geometry.

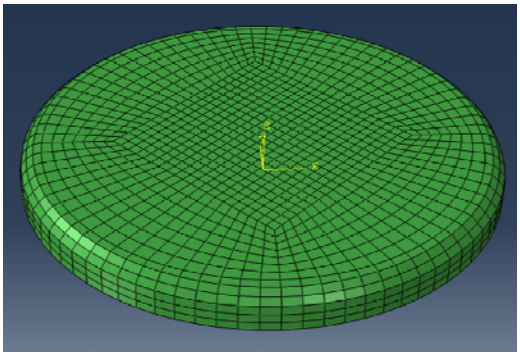

Figure 1: Meshed dynamically equivalent plate model

The fundamental nonlinear normal mode of the plate was computed from this model using the procedure discussed in [3, 4]. Specifically, a reduced order model was created using the Implicit Condensation method [12-14] and the nonlinear reduced order model (NLROM) was integrated in the NNMCont Matlab routine provided by Peeters, Kerschen, et al. [6] to compute the nonlinear modes. In [3, 4] this approach was found to provide an excellent approximation for the backbone of each NNM of a geometrically nonlinear beam. In the NLROMs presented here, only modes 1 and 6 are used as a modal basis since they are the first two symmetric modes with a nodal radius and hence both important to the response near the first natural frequency.

2.2 Experimental Structure

The article under investigation is a circular perforated plate with rolled ends which is shown in Fig. 2. A mechanical punch was used to create the circular perforations in a flat 16 gauge (1.52 mm thick) 409 stainless steel plate in an array of equilateral triangles with 10.16 mm long edges. Once this process was completed, the plate was formed around a 317.5 mm

diameter mold with the excess trimmed so a lip of 24.5 mm remained. The plate was then welded to an 89 mm high cylinder made from a 14 gauge (1.9 mm thick) 409 stainless steel plate that was cold rolled to the 317.5 mm diameter as shown in Fig. 2b. The welded plate assembly was then bolted to a fixture with twelve 6.4 mm evenly spaced holes. An 8000 N shaker was used to provide base excitation at a single harmonic to trace the nonlinear normal modes of the fundamental frequency of vibration. It is important to note that all stated dimensions are nominal and subject to variation as is observed in the final geometry of the two plates investigated here.

(a) **(b)**

Figure 2: Experimental setup of the perforated plates. a) Perforated plate before welding into test configuration, b) Perforated plate welded into the supporting cylinder.

The two plates considered for investigation are labeled perforated plate 1 (PP01) and perforated plate 2 (PP02). The initial geometry of both perforated plates were measured with 3D digital image correlation providing initial coordinates of the entire surface of the plates. The two plates presented here had an imperfect initial curvature induced by the method of formation as seen in Fig. 3. PP01 has an induced curvature with a peak deformation of 3.73mm when compared with the nominal model. This is shown in Figs. 3a & b, where the colormap segments the coordinate location of the measured surface. PP02 has an induced curvature with a peak deformation of 4.84 mm when compared with the nominal model as seen in Figs. 3c & d.

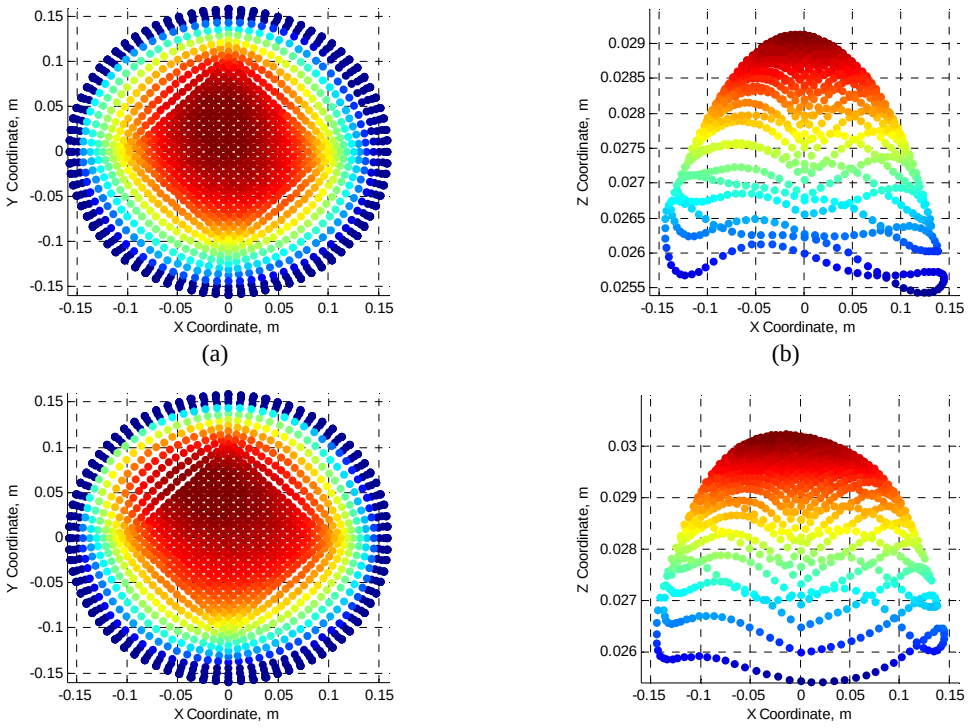

Figure 3: Measured initial geometry of the perforated plates. a) Front view of perforated plate 1 (PP01), b) side view

of perforated plate 1 (PP01), c) front view of perforated plate 2 (PP02), d) side view of perforated plate 2 (PP02).

3. Results

3.1 Model NNMs

Finite element models were created for each of these plates which are used to estimate the nonlinear normal mode (NNM) from a nonlinear reduced order model (NLROM) and are shown in Fig. 4 for the three models examined here. The frequency-energy plot (FEP), shown in Fig. 4a, highlights the difference in the energy dependence of the resonance frequency between the curved and flat models. The flat model (blue) exhibits only an increase in frequency as the amplitude of the response is increased, where PP01 (green) and PP02 (red) both show a decrease in frequency before an increase in frequency. The reason of this difference is further explained with the examination of the modal amplitudes shown in Fig. 4b. The flat model (blue) contains only the first mode of vibration in the dynamic response as the amplitude is increased. PP01 and PP02 both show a mode 1 dominance of the dynamic response as the frequency decreases; however, as the response reaches higher levels, the sixth mode begins to couple and takes a larger role in the dynamic response as the frequency increases. Although a different curvature is observed between PP01 and PP02, similar characteristics are observed in the dynamic response.

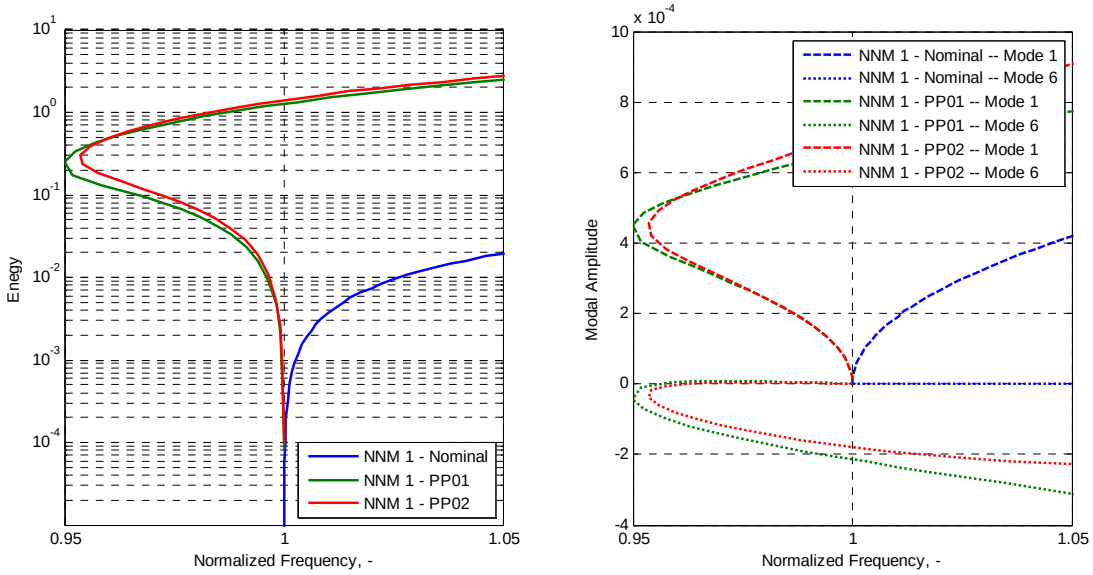

(a) (b)

Figure 4: Fundamental nonlinear normal mode of all models considered. a) frequency-energy plot of nonlinear reduced order model (NLROM), b) modal amplitudes of two-mode NLROM.

A further examination of the dynamic response also describes the harmonic coupling of the two mode NLROM. The response at the center of the plate at a change in frequency of +1% is shown in Fig. 5. As shown in the nominal model (blue) time domain, Fig. 5a, shows only a pure sinusoidal response while PP01 (green) and PP02 (red) shows a distortion in the time domain. Decomposing the signals into the frequency domain shows a single frequency in the nominal model response and multiple frequencies in PP01 and PP02. The higher frequency content points to a 1:3 harmonic coupling.

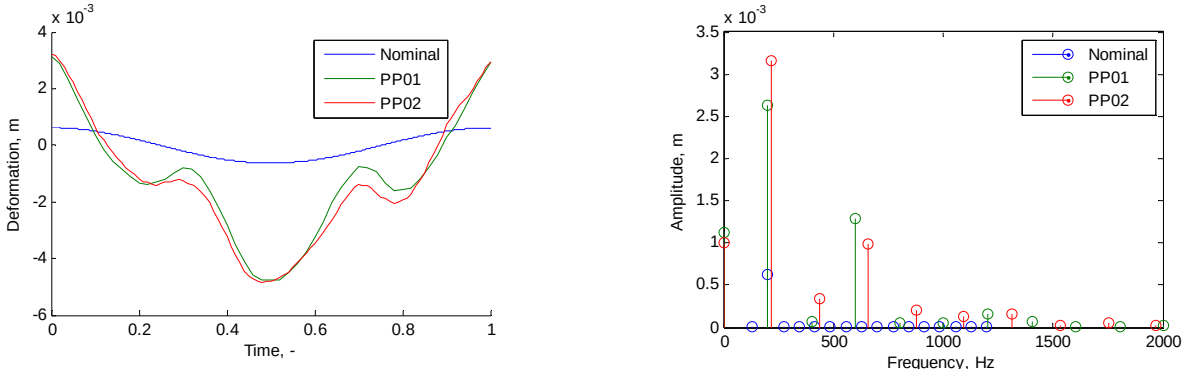

(a) (b)

Figure 5: NNM response at +1.0% increase of frequency. a) Time domain normalized to a period of the response, b) frequency domain.

Finally, an examination of the deformations observed at the peak harmonics in the response in the frequency domain provide a visualization of the modal coupling observed. Since the first harmonic is dominant in the nominal model and the first and third harmonic is dominant in PP01 and PP02 a comparison made between the full-field deformations of the plate at the same position on the FEP that was used in Fig. 5. The colorbars segment the out-of-paper deformations of the plate in meters. The first harmonic of the nominal model, shown in Fig. 6a, is purely a mode 1 deformation. Similarly, Fig. 6b & Fig. 6d, of the first harmonic of PP01 and PP02 which also resembles a mode 1 deformation. The third harmonic of PP01 and PP02 is also prominent in the response shown in Fig. 5. The deformation of the third harmonic of PP01 and PP02, shown in Fig. 6c & Fig. 6e, is a purely mode 6 deformation.

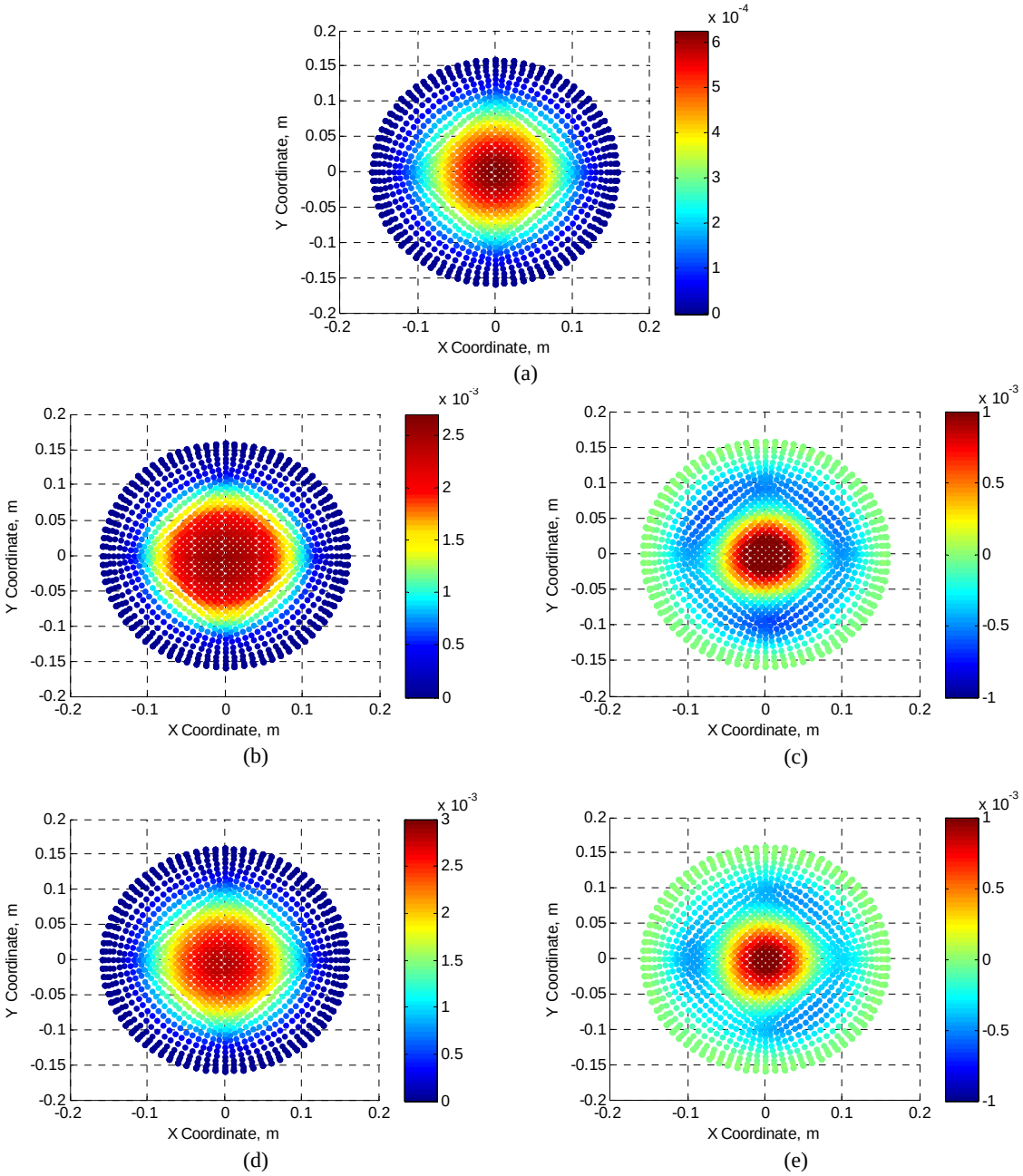

Figure 6: Deformation shapes of the peak harmonics at +1% of change in the fundamental frequency of vibration. a) Deformation of the fundamental harmonic of the nominal model, b) Deformation of the fundamental and c) third harmonic of PP01, d) Deformation of the fundamental and e) third harmonic of PP02.

3.2 Experimental NNMs

The experimentally measured NNMs are limited due to the experimental setup and the failure limit of the perforated plates tested. Therefore a complete examination of the NNM cannot be performed, as shown in Fig. 7, where the peak amplitude response of the center of the plate is plotted as a function of the resonance frequency. The decrease/increase of resonance frequency shown in Fig. 7 shows the ability of the NLROMs to capture the general trend of the nonlinear behavior of the perforated plates. The amplitude levels permitted by the experimental setup show an initial decrease in natural frequency larger than predicted by the numerical models for both plates. It is expected that as the response amplitude increases, the plate may pull on the external rim of the setup, requiring larger response amplitudes before the axial stretching reaches levels capable of changing the nonlinearity from a softening to hardening effect. The turning point can be captured experimentally; however the failure occurs as the change in frequency begins to increase limiting the full characterization of the increase in frequency.

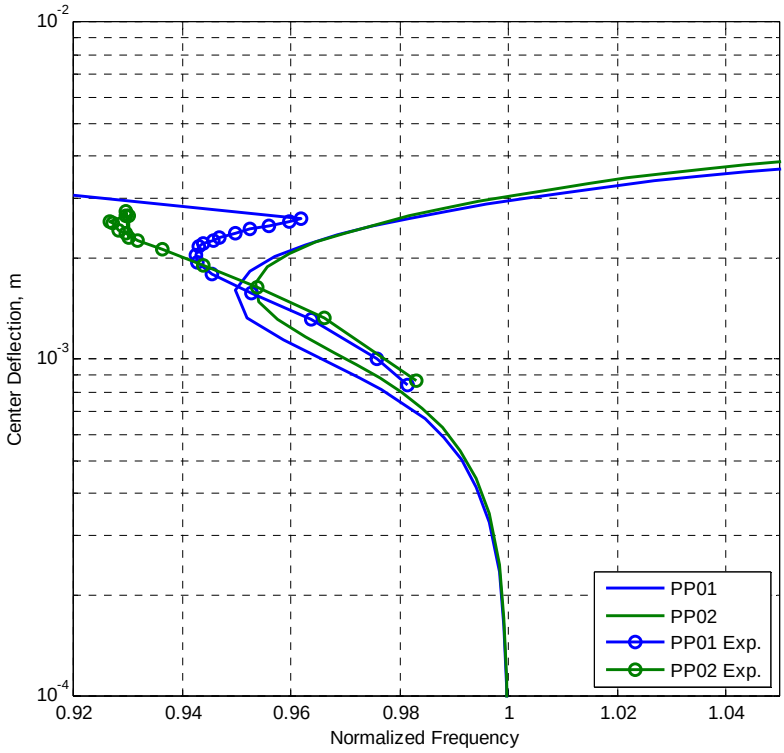

Figure 7: Peak amplitude at center of plate.

The full field deformation at the point where the change in the fundamental frequency of vibration provides a good comparison of the dynamic response in nonlinear regimes as shown in Fig. 8. The colorbar accompanying each figure corresponds to the peak deformation observed in the full-field deformation. The full-field deformations observed for the modeled PP01, shown in Fig. 8a-b, has a peak deformation of 1.67mm for the first harmonic and 0.29mm for the third harmonic. The companion experimental deformations are shown in Fig. 8c-d, where a peak deformation of 1.94mm is measured for the first harmonic and 0.41mm for the third harmonic. The first harmonic for this structure is 16% higher than predicted by the model, and the third harmonic is 40% higher. The full-field deformations for PP02, shown in Fig. 8e-f, has a peak amplitude of 1.78mm for the first harmonic and 0.27mm for the third harmonic. The experimental deformations are shown in Fig. 8g-h, where a peak deformation of 2.43mm is observed for the first harmonic and a peak deformation of 0.23mm is observed for the third harmonic. The first harmonic for this structure is 36% greater than that predicted by the model and the third harmonic is 17% lower than predicted by the model. The difference between the harmonic amplitudes of the models suggest a modal coupling not accounted for in the NLROM. A further examination of the higher harmonics of the experimental setup is needed to characterize the modal coupling and will guide the next step in the creation of NLROMs. One interesting thing to note is the asymmetry in the third harmonic shown in Fig. 8h, which is not as pronounced in the experimental results, and could be a result of the base excitation loading which limits the ability to excite asymmetries in the structure fully.

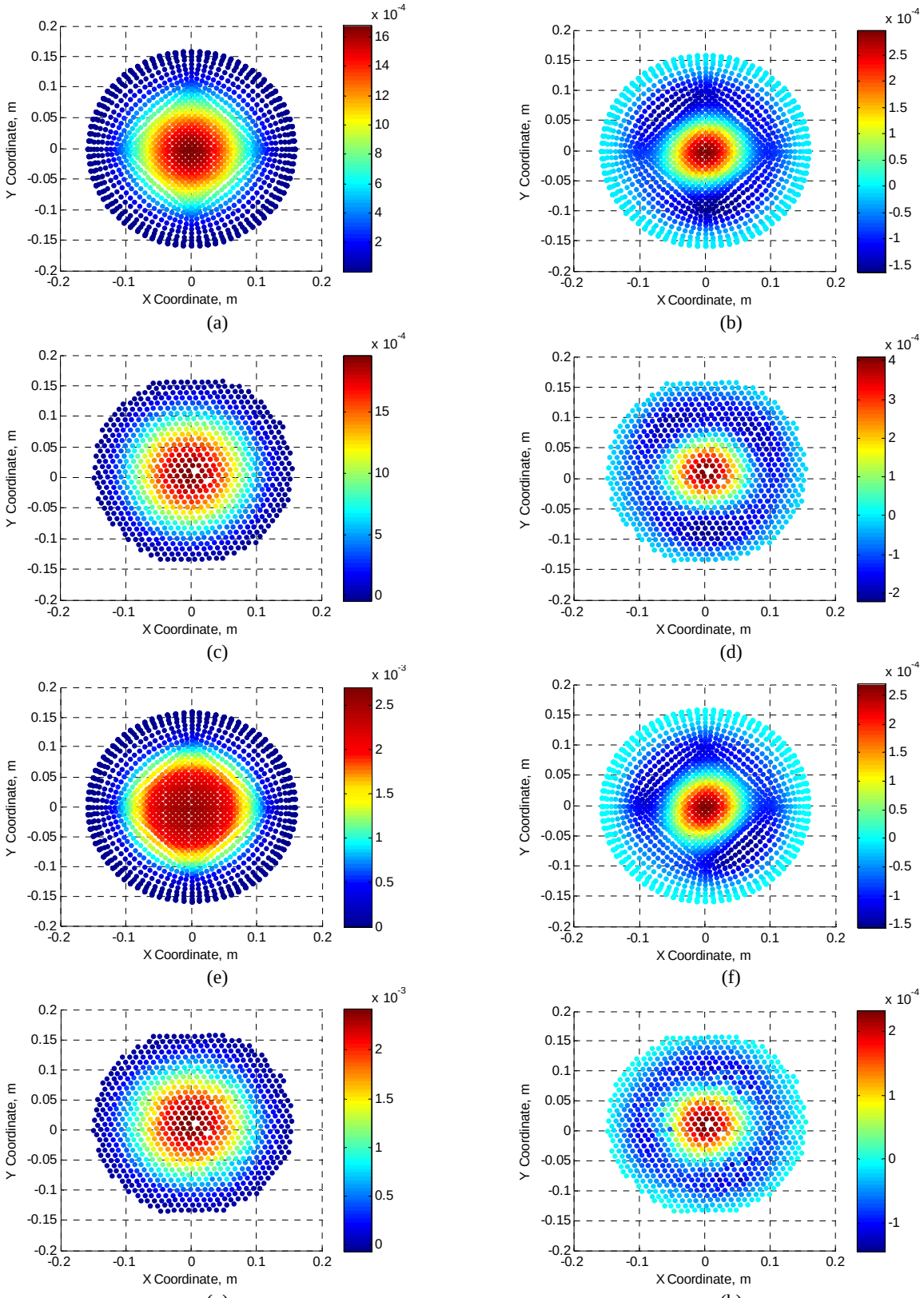

Figure 8: Full field deformations of the perforated plates. PP01 first and third harmonic of the a-b) numerically calculated and of the c-d) experimentally measured point of maximum decrease in frequency. PP02 first and third harmonic of the a-b) numerically calculated and of the c-d) experimentally measured point of maximum decrease in frequency.

4. Conclusion

The examination of the nonlinear normal modes (NNMs) has provided insight to the underlying modal and harmonic coupling observed in the perforated plates investigated. The nominal model, assuming a flat geometry, showed only an increase in the fundamental frequency of vibration as the response amplitude is increased. With the inclusion of the initial curvature of the perforated plates, a strong coupling is observed between mode 1 and mode 6 of the plate for the first NNM. Therefore, the inclusion of mode 1 and mode 6 into the nonlinear reduced order models is needed. As the structure is pushed at higher input forces the mode 6 deformation becomes more pronounced as shown experimentally and numerically. Although more tuning is needed to accurately account for the amount of coupling between mode 1 and mode 6.

Though the models have shown the ability to describe the trend of the dynamic behavior of the perforated plates, more work is needed to fully identify the modal coupling in the experimental results. Additionally, an examination of the stress distribution of the change in deformation observed in the plates is needed for accurate prediction of the failure of these plate.

References

1. Kerschen, G., et al., *Nonlinear normal modes, Part I: A useful framework for the structural dynamicist.* Mechanical Systems and Signal Processing, 2009. **23**(1): p. 170-194.
2. Peeters, M., et al., *Nonlinear normal modes, part II: toward a practical computation using numerical continuation techniques.* Mechanical Systems and Signal Processing, 2009. **23**(1): p. 195-216.
3. Allen, M.S., et al., *A Numerical Continuation Method to Compute Nonlinear Normal Modes Using Modal Reduction*, in *53rd AIAA Structures, Structural Dynamics, and Materials Conference*. 2012: Honolulu, Hawaii.
4. Kuether, R.J. and M.S. Allen, *A Numerical Approach to Directly Compute Nonlinear Normal Modes of Geometrically Nonlinear Finite Element Models.* Mechanical Systems and Signal Processing, 2013.
5. Gordon, R.W.a.H., J.J., *Reduced Order Models for Acoustic Response Prediction*. 2011, Air Force Research Laboratory.
6. Peeters, M., G. Kerschen, and J.C. Golinval, *Dynamic testing of nonlinear vibrating structures using nonlinear normal modes.* Journal of Sound and Vibration, 2011. **330**(3): p. 486-509.
7. Peeters, M., G. Kerschen, and J.C. Golinval, *Modal testing of nonlinear vibrating structures based on nonlinear normal modes: Experimental demonstration.* Mechanical Systems and Signal Processing, 2011. **25**(4): p. 1227-1247.
8. Ehrhardt, D.A., *A Full-Field Experimental and Numerical Investigation of Nonlinear Normal Modes in Geometrically Nonlinear Structures*, in *Engineering Mechanics*. 2015, University of Wisconsin-Madison.
9. Kuether, R.J. and M.S. Allen, *Computing Nonlinear Normal Modes Using Numerical Continuation and Force Appropriation*, in *ASME 2012 International Design Engineering Technical Conferences IDETC/CIE 2012*. 2012: Chicago, IL.
10. Ehrhardt, D.A., Allen, M.S., Yang, S., and Beberniss, T.J.,, *Full-Field Linear and Nonlinear Measurements using Continuous-Scan Laser Doppler Vibrometry and High Speed Three-Dimensional Digital Image Correlation.* Mechanical Systems and Signal Processing, 2015. **In Review**.
11. Jo, M.J.J.a.J.C., *Equivalent Material Properties of Perforated Plate with Triangular or Square Penetration Pattern for Dynamic Analysis.* Nuclear Engineering and Technology, 2006. **38**(7).
12. Gordon, R.W. and J.J. Hollkamp, *Reduced-order Models for Acoustic Response Prediction*. 2011, Air Force Research Laboratory: Dayton, OH.
13. Hollkamp, J.J. and R.W. Gordon, *Reduced-order models for nonlinear response prediction: Implicit condensation and expansion.* Journal of Sound and Vibration, 2008. **318**(4-5): p. 1139-1153.
14. Hollkamp, J.J., R.W. Gordon, and S.M. Spottswood, *Nonlinear modal models for sonic fatigue response prediction: a comparison of methods.* Journal of Sound and Vibration, 2005. **284**(3-5): p. 1145-63.